

Mechanically Programmed Self-Folding at the Millimeter Scale

Samuel M. Felton¹, Michael T. Tolley¹, and Robert J. Wood¹

Abstract—Self-folding enables the fabrication of sophisticated shapes from planar materials without manual assembly. This capability is valuable at millimeter scales, where traditional manufacturing is difficult and expensive, and MEMS techniques are not well-suited to 3-D features with high aspect ratios. Automating the assembly process through self-folding also has the potential to speed up the manufacturing time and reduce labor costs. However, existing self-folding techniques are not capable of complex geometries at the millimeter scale. In this paper we present a self-folding composite that is capable of complex sub-centimeter structures and mechanisms. The self-folding pattern is mechanically programmed into the composite during fabrication, and folding is activated by heating the composite. We show that this technique is capable of feature sizes ranging from 1 to 20 mm, and can create both shapes and mechanisms. We demonstrate this with two self-folding pieces: a cube and a spherical five-bar linkage. These results demonstrate the potential for self-folding systems to be integrated with MEMS fabrication techniques to produce complex devices.

I. INTRODUCTION

Self-folding is a form of self-assembly in which a planar material or composite transforms itself into a three-dimensional structure by bending along hinges. It is capable of achieving complex geometries at a wide range of size scales compared to other forms of self-assembly. Various approaches have achieved hinges shorter than 100 μm [1], [2], and feature sizes greater than 10 cm [3]. Self-folding is also achievable with a variety of actuation methods, including polymer films [1], external magnetic fields [2], shape memory alloy actuators [4], and prestressed layers [5].

There are many advantages to using origami-inspired manufacturing methods such as self-folding. Computational algorithms and tools can automatically produce planar fold patterns from a desired three-dimensional structure [6], [7], and design linkage systems from a desired kinematic path [8], [9]. Folded structures also have advantages inherent to their structure, such as higher strength-to-weight ratios, and a variety of origami-inspired devices demonstrate these benefits [10], [11], [12]. Folding can even be used as a form of printable manufacturing by exploiting the speed and low cost of planar fabrication techniques to rapidly and cheaply produce a laminate which can then be folded into a functional machine [13].

Self-folding is also valuable for fabrication at the millimeter and micrometer scales, where manual assembly is difficult. Manufacturing complex sub-centimeter structures

¹School of Engineering and Applied Sciences, Harvard University, Cambridge, MA 02138, USA, and the Wyss Institute for Biologically Inspired Engineering, Harvard University, Boston, MA 02115, USA. sam@seas.harvard.edu

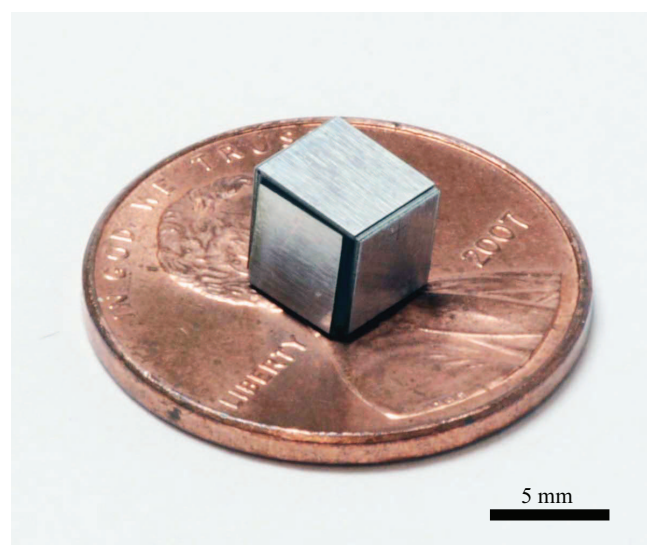


Fig. 1. A five-millimeter self-folding cube. This structure was fabricated as a flat composite and assembled itself when it was heated above 130°C.

is a challenge for existing manufacturing techniques. Traditional machining methods are suited for features at the centimeter scale and larger, but become imprecise and time consuming for smaller geometries. MEMS techniques are capable of producing micrometer and millimeter scale features using surface machining and monolithic materials, but are ill-suited to larger structures or complex shapes with different constituent materials. This hole in manufacturing capabilities has already been addressed with one self-folding technique: Pop-Up Book MEMS has demonstrated the ability to create centimeter-long machines using composites [14], [15]. However, this technique has its own drawbacks. The folding process occurs in a single step, which restricts possible geometries [16], and requiring substantial design time and skill to achieve the appropriate folding patterns. It also requires extra scaffold material, extra joints for out-of-plane features, and an additional fixing step to lock pop-up joints into place. Other microscale self-folding techniques face different challenges: Soft polymers often require specific and impractical environments, such as aqueous environments with particular pH levels [1]. Light- or laser-activated folding requires line-of-sight to all folding hinges, as well as external machinery [17], [18].

In this paper we present a method for practical and robust self-folding at the millimeter scale (Fig. 1). This technique relies on shape memory composites - structural substrates bonded to shape memory polymers which contract when activated. This contraction causes the composite to bend at

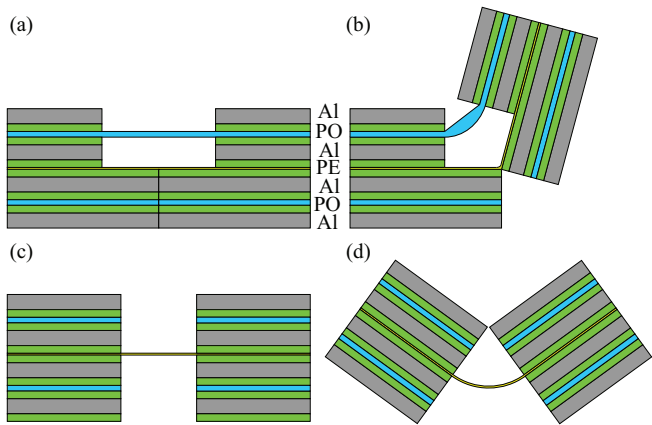


Fig. 2. The self-folding composite consists of aluminum (AL, gray), polyolefin (PO, blue), polyester (PE, yellow), and cyanoacrylate adhesive (green). A diagram of a self-folding hinge is shown before (a) and after (b) activation. This composite is also capable of bidirectional flexure hinges (c-d) for dynamic mechanisms.

a pre-programmed hinge, creating a fold. A fold pattern is mechanically programmed into the composite that results in an arbitrarily specified three-dimensional shape. SMCs have already been used to create structures and machines with centimeter-scale features [3], [19], [20], [21]. These composites are capable of sequential or simultaneous folds and bidirectional angle-controlled folding. They are also capable of creating linkage mechanisms, and can be easily integrated with planar sensors [22]. However, they are incapable of producing features that are less than a centimeter long. This is because the SMP delaminates off of faces with areas less than a square centimeter and the thickness of these composites limits the minimum distance between folds. In this work, we determine new materials and fabrication techniques to create a composite capable of self-folding hinges as short as one millimeter. We demonstrate that the self-folding hinges can be mechanically programmed to fold to specific angles, and demonstrate its ability to produce shapes and mechanisms by folding a cube and a spherical five-bar linkage.

II. DESIGN AND MODEL

The composite used in this paper is similar to previous shape memory composites [3], [20]. A contractile layer and structural substrate are bonded to form a bimorph actuator, which bends when the contractile layer is activated (Fig. 2). This bending is concentrated into a fold by weakening the substrate along a line.

The contractile layer used in these composites is a shape memory polymer (SMP), a material which undergoes a preprogrammed shape change when it is heated above its glass transition temperature, T_g [23]. When heated above this temperature, the SMP transforms from a glass state to a rubbery state, and it undergoes a simultaneous change of its resting shape and its mechanical properties. In its glassy state, the SMP has an elastic storage modulus on the order of 10-3000 MPa. In its rubbery state, the elastic

storage modulus, also known as the rubbery modulus, is on the order of 0.1-10 MPa [24]. Because its resting state has changed, the material experiences an internal stress if held in place, as the effective strain in the material changes. In this application, we use an SMP that has been programmed to shrink bidirectionally to 25% of its original length and width (also known as a shrink ratio of 4:1). This type of SMP is commonly available as shrink wrap.

In the following experiments, heat is applied to the structure uniformly by an oven (Isotemp model 282A, Fisher Scientific), activating all of the hinges simultaneously. When the hinges are cooled, the SMP stiffens and the hinge becomes static. Bidirectional folding is made possible by including contractile layers on both sides of the composite, and a polymer thin film runs through the center of the composite, acting as a flexural layer for both actuated and passive hinges. In previous examples of shape memory composites, the minimum feature size was limited by delamination of the contractile layer from the substrate [3]. To mitigate this, the composite presented here includes two additional substrate layers on the outside of the contractile layers to inhibit SMP peeling. This has the added benefits of increasing stiffness and maintaining a uniform outer surface.

We chose to use the following materials in our composite: 50 μm aluminum (AL) as the substrate because of its high stiffness-to-weight ratio; 18 μm polyolefin (PO) as the SMP because it is non-toxic and commercially available as heat shrink wrap; and 2.5 μm polyester (PE) as the flexural layer because it is thin and flexible. A cyanoacrylate adhesive (CA) was used to bond each layer together. Therefore, the final laminate consists of two similar sublaminate composed of AL and PO (AL-CA-PO-CA-AL) on either side of a flexural layer (CA-PE-CA).

Actuated hinges in the laminate are created by cutting a gap with an arbitrary width in the two substrate layers on the concave side, and cutting a line in the substrate and SMP layers on the convex side (Fig. 2a-b). Passive hinges are created by cutting a gap in the substrate and SMP layers on both sides of the laminate, leaving only the flexural layer. The stiffness is adjusted by varying the length and gap width of the hinge.

The final angle of an actuated hinge is mechanically

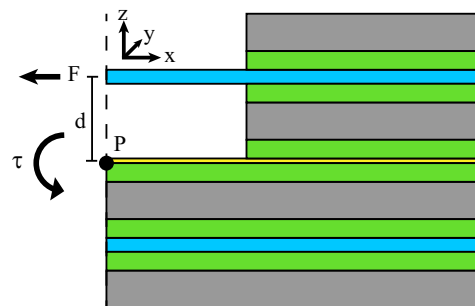


Fig. 3. Torque is caused by the force F due to the stress of the SMP while contracting, as well as the lever arm d of the SMP layer from the point of rotation P , which is the intersection of the flexural layer and the hinge line.

TABLE I
MATERIAL AND COMPOSITE PROPERTIES

PO rubbery modulus	E	550 kPa
PO Poisson's ratio	ν	0.5
PO thickness	t_p	19 μm
Composite thickness	t_c	300 μm
Lever arm	d	80 μm
Torque-per-meter	τ/w	82 μm
Area density	ρ_a	1.88 kg/m ²
In-plane strain	ϵ_x, ϵ_y	3
Out-of-plane stress	σ_z	0
In-plane stress	σ_x, σ_y	3.3 MPa
Maximum face length	l_{max}	73 mm
PO transition temperature	T_g	130°C
Specific heat capacity	c_p	900 J/kgK
Thermal contact conductivity	h_c	1000 W/m ² K

programmed into the laminate, similar to the method shown previously by Tolley et al. [21]. The final angle varies with the gap width of the substrate on the concave side. As the hinge folds, the substrate on either side of the hinge comes closer together (Fig. 2b). The farther apart the two edges of the substrate are, the farther the hinge can fold before they come into contact. The relationship between gap width w_g , composite thickness t_c , and fold angle θ is given as

$$\theta = 180^\circ - \arctan\left(\frac{t_c}{w_g}\right) \quad (1)$$

There is an upper limit to how big the self-folded object can be due to gravity. If the hinge cannot apply sufficient torque to lift the folding face, the SMP will eventually break. The maximum feature size is defined by the hinge torque, which is dependent on the material and composite properties, specifically the width w , the thickness t_p , and the Young's modulus E of the SMP. These can be used to determine the stress σ_x in the SMP after activation that's in plane with the sheet and perpendicular to the hinge, and the force F in the same direction. It also depends on the distance d between the SMP and the center of the composite (Fig. 3). For a given composite, these values do not change, limiting the maximum possible face size for a given composite. The torque τ exerted by a hinge is

$$\tau = Fd = \sigma_x w t_p d \quad (2)$$

Because the PO used in this composite has a shrink ratio of 4:1, we assume the SMP layer is undergoing strains ϵ_x and ϵ_y of 3 while in a rubber state. The stress is then calculated using Hooke's Law.

$$\epsilon_x = 3 = (1/E)(\sigma_x - \sigma_y \nu - \sigma_z \nu) \quad (3)$$

$$\epsilon_y = 3 = (1/E)(\sigma_y - \sigma_x \nu - \sigma_z \nu) \quad (4)$$

$$\sigma_x = 6E \quad (5)$$

E and ν are the Young's modulus and Poisson's ratio of the SMP. We can characterize the maximum face size a hinge can lift by considering the simplified case of a rectangular face.

The maximum size of this face is defined by the maximum length of the face l_{max} extending orthogonally from the hinge line. By combining equations (2) and (5) with the properties of the composite (Table I), we can estimate l_{max} .

$$6E w t_p d = w l_{max}^2 \rho_a / 2 \quad (6)$$

$$l_{max} = \sqrt{\frac{12E t_p d}{\rho_a}} \quad (7)$$

For the composite used in this paper, we calculate that the maximum face length is 73 mm. It's worth noting that this limit assumes a contiguous, rectangular face. The maximum feature size can be increased cutting windows into the face, removing material and reducing weight.

The time required to fold these composites is expected to be less than one minute because the composite can be rapidly heated. The time this takes in an oven can be predicted by assuming that conduction within the composite occurs more quickly than heat transfer into the composite and that conduction between the ceramic floor of the oven and the composite is greater than the heat flux due to convection and radiation. This allows us to use a lumped thermal model to express the energy transfer rate \dot{Q} as a function of the surface area A , time varying temperature T , and thermal contact conductivity h_c of the composite, as well as the constant temperature T_o of the oven. h_c was estimated from the calculations of Yovanovich et al. [25].

$$\dot{Q} = h_c A (T_o - T) \quad (8)$$

We can also express the temperature in terms of the initial temperature T_i , the total energy transfer Q , and the total heat capacity of the composite, which is dependent on the composite volume V , lump density ρ , lump specific heat capacity c_p .

$$(T - T_i) = \frac{Q}{\rho V c_p} \quad (9)$$

Equations (8) and (9) can be combined into a differential equation, and the temperature can be solved explicitly as a function of time.

$$\frac{\rho_a c_p}{h_c} \dot{T} = T_o - T \quad (10)$$

$$T = (T_i - T_o) \exp\left(-t \frac{h_c}{\rho_a c_p}\right) + T_o \quad (11)$$

The time required for the activation of self-folding is the time it takes for T to reach the glass transition temperature T_g of the composite, when folding is activated.

$$t = \frac{\rho_a c_p}{h_c} \log\left(\frac{T_i - T_o}{T_g - T_o}\right) \quad (12)$$

Here we assume that the composite's initial temperature T_i is the room temperature, 20°C, the oven temperature T_o is 140°C, and the transition temperature T_g is 130°C. Because of this, we expect folding to occur within five seconds of contact with the ceramic surface.

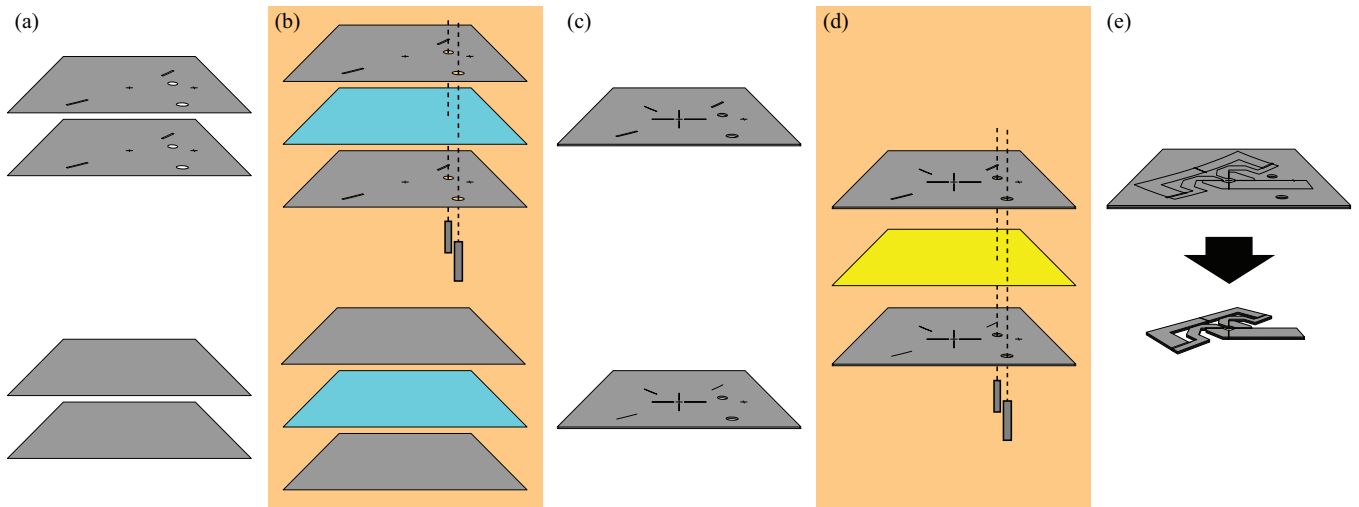


Fig. 4. The fabrication process occurs in five steps. Shown here is the fabrication of a spherical five-bar linkage. (a) Four aluminum layers are laser-machined with layer specific patterns. This results in two identical upper layers and two identical lower layers. In the case of this linkage, the lower aluminum layers require no cutting. (b) The aluminum layers are spincoated with adhesive and bonded to either side of a polyolefin layer, resulting in an upper composite and a lower composite. (c) Each composite is laser-machined with more layer-specific features. (d) These composites are spincoated with adhesive, and bonded to either side of a polyester thin film. (e) The complete composite is laser-machined into the final planar form.

III. FABRICATION

Each self-folding laminate is assembled in five steps. First, each of four aluminum layers (Shim-In-A-Can, Shop-Aid) is machined with layer-specific features (Fig. 4a) using a diode-pump solid-state laser (DC150H-355, Photonics Industries). A cyanoacrylate adhesive (496, Loctite) is spincoated onto each aluminum layer and these layers are bonded to either side of a sheet of prestretched polyolefin (Sytec MVP 75 G, Syfan), using pins to align the layer features (Fig. 4b). This results in a top and bottom composite, each comprising one polyolefin and two aluminum layers. These composites are then laser-machined again with additional features such as cuts through the polyolefin layers (Fig. 4c). Adhesive is spincoated on each composite, and these are pin aligned and bonded to either side of a polyester thin film sheet (Cat. No: 100, Chemplex; Fig. 4d). The full laminate is laser-machined again to release the desired mechanism (Fig. 4e).

For example, in order to create a single 90° self-folding hinge, we first cut a 0.5 mm gap in two AL layers along the length of the hinge. We then spincoat adhesive on these two AL layers, lay a single layer of PO between them, align them with pins, and bond them together. We also spincoat adhesive onto two uncut AL layers and bond them to either side of another layer of PO. After curing, we cut a single line into the second AL-PO-AL composite along the hinge. We then spincoat adhesive onto each AL-PO-AL composite and bond them to either side of a PE layer, aligning the two composites with pins.

IV. EXPERIMENTS AND RESULTS

We built self-folding hinges with uniform face size and varying gap width to determine the relationship between substrate gap width and final fold angle. Each folding face was five millimeters long by five millimeters wide, with a

gap width on the concave aluminum layers of 0.2 to 0.8 mm. We placed five samples for each gap width in an oven preheated to $140 - 150^\circ \text{C}$ for 45 s in order to ensure complete folding. Figure 5 compares the experimental results with the predictive model given in eq. 1. The data indicates a positive correlation between gap width and fold angle.

We built self-folding hinges with square faces that varied in size from 1 to 20 mm long. The 1 mm, 2 mm, 4 mm, and 20 mm faces all folded successfully (Fig. 6). The 3 mm face failed to fold because the AL delaminated from the PO during folding, and was subsequently removed. Due to the torque model presented earlier, we believe larger features could be folded, but our laser machining system

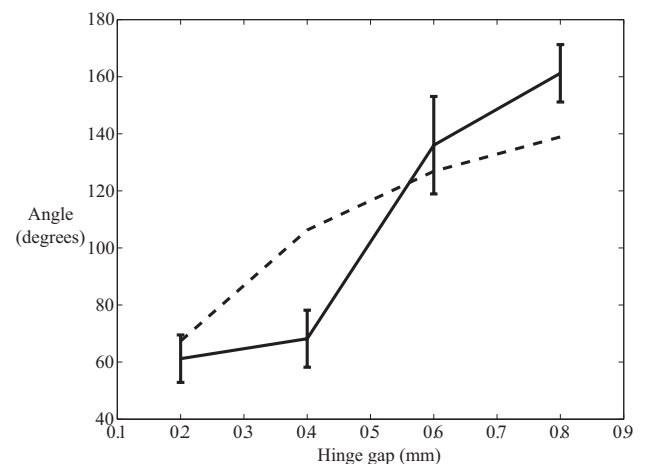


Fig. 5. The experimental data (solid line) and model (dashed line) relating the gap width in the substrate to the final fold angle of self-folding hinges. Five hinges were tested and measured with each gap width. Error bars indicate the standard deviation.

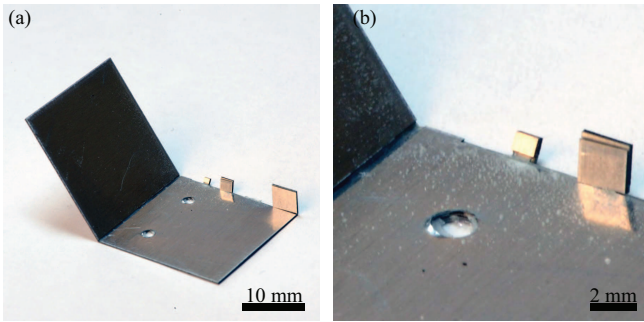


Fig. 6. Self-folding hinges were built that were 1 mm, 2 mm, 3 mm, 4 mm, and 20 mm in order to determine the maximum and minimum feature sizes this self-folding technique was capable of creating. All hinges successfully self-folded except the 3 mm hinge, which delaminated during the folding process. This indicates that the spatial resolution of this technique is at least 1 mm.

has a maximum work space which limits the possible size of a symmetrical hinge to less than 25 mm.

We built a self-folding cube to demonstrate the ability of this method to produce shapes (Fig. 7, Supp. Video). The unfolded version of this structure was placed into an oven preheated to between 140 – 150° C for 20 s, until folding was completed. The cube weighed 80 mg.

We fabricated a spherical five-bar linkage using this self-folding technique to demonstrate the ability to produce complex mechanisms (Fig. 8, Supp. Video). This linkage has two degrees of freedom and transforms two angular inputs into one or two decoupled angular outputs. This linkage is based on a similar one demonstrated by Sreetharan et al. [15] and used in multiple microrobotic designs [26], [27]. The design requires five dynamic hinges to be arranged so that their coincident lines intersect at a single point. The unfolded version of this linkage was placed into an oven preheated to between 140 – 150° C for 20 s, during which the out-of-plane component of the linkage folded into place. Afterwards, the ability of the linkage to transmit an angular displacement from one linkage to another was verified by applying a torque to one linkage with tweezers (Supp. Video). The mechanism weighed 120 mg. After the torque was removed, the linkage returned to its resting state, indicating that the flexural hinges behaved elastically.

V. DISCUSSION

The self-folding method presented here has demonstrated the ability to create shapes and mechanisms with millimeter-

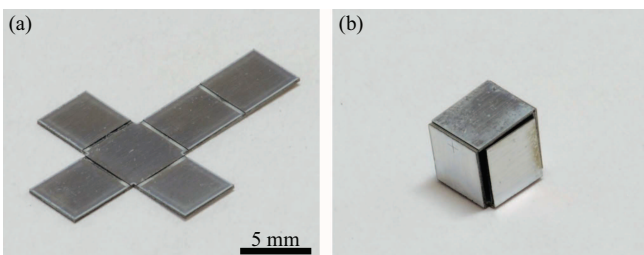


Fig. 7. A five-millimeter self-folding cube before (a) and after (b) folding.

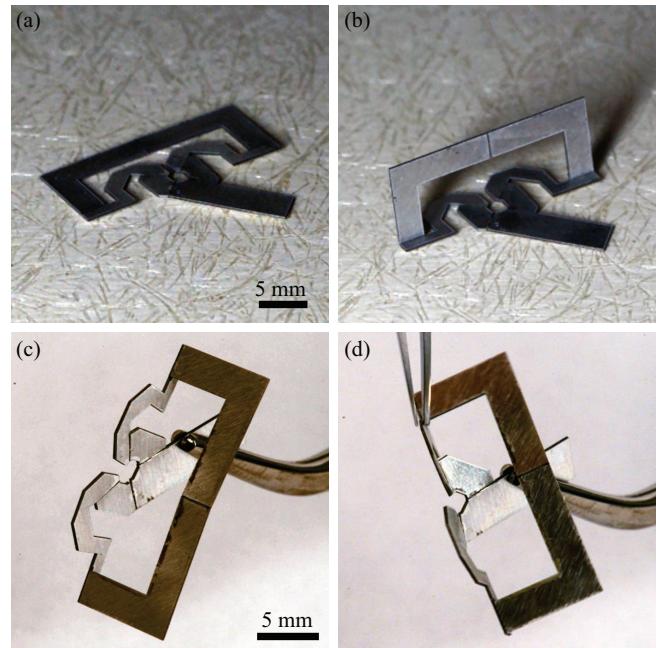


Fig. 8. A spherical five-bar linkage was fabricated using this self-folding technique. (a) The planar form of the linkage in the oven. (b) The linkage after folding is complete. (c) The linkage in its resting state. (d) The articulated linkage.

scale features. The ability to fold a one millimeter square face indicates the ability to create shapes at a millimeter-scale resolution, while the model predicts we could fold similar features 70 times this size with appropriate fabrication facilities. The cube demonstrates that these lessons can be used to create shapes, while the spherical linkage shows that the technique is also capable of dynamic mechanisms.

This fabrication process still has a limit on the minimum feature size that can be achieved. The total composite thickness is approximately 300 μm , and the aluminum accounts for 200 μm of that. A thinner, stiffer substrate such as steel or carbon fiber would result in a thinner substrate. Alternatively, a sufficiently strong adhesive would make the outer substrate layer unnecessary, reducing the composite thickness by 100 μm . The minimum surface area of the folding faces is limited by adhesion as well. Smaller faces have less surface area for binding and are more prone to separation. This occurred in the three millimeter face in figure 6, but could be prevented by more reliable adhesive methods, since in some cases even smaller faces folded successfully. In addition, as hinges become smaller, off-axis effects such as twisting become more likely at the hinges, particularly as the hinge length becomes equal to the composite thickness.

The relation between gap width and fold angle indicates a way to mechanically program the final geometry into the 2D composite. However, the current method still exhibits substantial variation in final angle for a given gap width, and does not match the analytical model closely. We believe this error is due to two factors. First, we believe that individual layers are slipping during the folding process, altering the hinge geometry. Since we have already witnessed

delamination, it is reasonable that other, less visible defects are occurring. The second possible cause for angle variation is misalignment of the substrate edges on either side of the hinge. Our analytical model assumes that the substrates touch at their respective corners, but a slight misalignment would result in the corner of one side contacting a flat surface on the other, altering the final angle. This may be preventable with sloped or rounded edges.

We believe that these limitations and defects are due primarily to insufficient bonding of the polyolefin to the metal. Polyolefin was chosen because of its non-toxicity and compatibility with laser-machining, but it is also known for having low surface energy, and consequently is difficult to bond. Commercial polyolefin adhesives exist, but they are not compatible with our spincoating process. Further research will improve the bonding process through the use of new adhesives and fabrication techniques.

The model could also be refined. The variable temperature, viscoelastic effects, and high strain all complicate analytical predictions of the solid mechanics. If this technique were to be applied in a commercial setting, we recommend extensive characterization in order to optimize material selection and heat application.

This fabrication method has potential for constructing complex machines at the sub-centimeter scale. It can create the sophisticated mechanisms used in microrobots [26], [27], or mass-produce miniature surgical devices [28]. Because it relies on planar laminates, it can take advantage of the small size and cost of MEMS devices while incorporating the complex mechanisms seen in traditionally manufactured machines. Because it requires only a laser cutter and a spincoater, devices can be fabricated from digital plans without a large capital investment. Finally, self-folding could enable on-site assembly, in which sheets of pre-programmed composites are easily packaged and shipped, and then transform into functional devices after arriving at their destination.

ACKNOWLEDGMENT

The authors gratefully acknowledge support from the National Science Foundation (award numbers CCF-1138967 and EFRI-1240383) and the DoD, Air Force Office of Scientific Research, National Defense Science and Engineering Graduate (NDSEG) Fellowship, 32 CFR 168a. Any opinions, findings, and conclusions or recommendations expressed in this material are those of the authors and do not necessarily reflect those of the National Science Foundation.

REFERENCES

- [1] L. Ionov, "Soft microorigami: self-folding polymer films," *Soft Matter*, vol. 7, no. 15, pp. 6786–6791, 2011.
- [2] Y. W. Yi and C. Liu, "Magnetic actuation of hinged microstructures," *Journal of Microelectromechanical Systems*, vol. 8, no. 1, pp. 10–17, 1999.
- [3] S. M. Felton, M. T. Tolley, B. Shin, C. D. Onal, E. D. Demaine, D. Rus, and R. Wood, "Self-folding with shape memory composites," *Soft Matter*, 2013.
- [4] E. Hawkes, B. An, N. M. Benbernou, H. Tanaka, S. Kim, E. D. Demaine, D. Rus, and R. J. Wood, "Programmable matter by folding," *Proceedings of the National Academy of Sciences*, vol. 107, no. 28, p. 12441, 2010.
- [5] N. Bassik, G. M. Stern, and D. H. Gracias, "Microassembly based on hands free origami with bidirectional curvature," *Applied physics letters*, vol. 95, no. 9, pp. 091901–091901, 2009.
- [6] E. D. Demaine, M. L. Demaine, and J. S. B. Mitchell, "Folding flat silhouettes and wrapping polyhedral packages: New results in computational origami," *Computational Geometry*, vol. 16, no. 1, pp. 3–21, 2000.
- [7] T. Tachi, "Origamizing polyhedral surfaces," *Visualization and Computer Graphics, IEEE Transactions on*, vol. 16, no. 2, pp. 298–311, 2010.
- [8] M. Kapovich and J. J. Millson, "Universality theorems for configuration spaces of planar linkages," *Topology*, vol. 41, no. 6, pp. 1051–1107, 2002.
- [9] T. G. Abbott, E. D. Demaine, and B. Gassend, "A generalized carpenter's rule theorem for self-touching linkages," *arXiv preprint arXiv:0901.1322*, 2009.
- [10] K. Miura, "Method of packaging and deployment of large membranes in space," in *31st Congress of the International Astronautical Federation*, 1980.
- [11] L. L. Howell, *Compliant mechanisms*. Wiley-Interscience, 2001.
- [12] P. S. Gollnick, S. P. Magleby, and L. L. Howell, "An introduction to multilayer lamina emergent mechanisms," *Journal of Mechanical Design*, vol. 133, p. 081006, 2011.
- [13] C. D. Onal, R. J. Wood, and D. Rus, "Towards printable robotics: Origami-inspired planar fabrication of three-dimensional mechanisms," in *IEEE Int. Conf. on Robotics and Automation (ICRA)*. IEEE, 2011, pp. 4608–4613.
- [14] J. P. Whitney, P. S. Sreetharan, K. Y. Ma, and R. J. Wood, "Pop-up book MEMS," *Journal of Micromechanics and Microengineering*, vol. 21, no. 11, p. 115021, 2011.
- [15] P. S. Sreetharan, J. P. Whitney, M. D. Strauss, and R. J. Wood, "Monolithic fabrication of millimeter-scale machines," *Journal of Micromechanics and Microengineering*, vol. 22, no. 5, p. 055027, 2012.
- [16] R. Uehara and T. Sachio, "The complexity of a pop-up book," Japan Advanced Institute of Science and Technology, Tech. Rep. 2006-AL-107 (10), 2006.
- [17] Y. Liu, J. K. Boyles, J. Genzer, and M. D. Dickey, "Self-folding of polymer sheets using local light absorption," *Soft Matter*, vol. 8, no. 6, pp. 1764–1769, 2012.
- [18] K. E. Laffin, C. J. Morris, T. Muqem, and D. H. Gracias, "Laser triggered sequential folding of microstructures," *Applied Physics Letters*, vol. 101, no. 13, pp. 131901–131901, 2012.
- [19] S. M. Felton, M. T. Tolley, C. D. Onal, D. Rus, and R. J. Wood, "Robot self-assembly by folding: A printed inchworm robot," in *Robotics and Automation (ICRA), 2013 IEEE International Conference on*. IEEE, 2013, pp. 277–282.
- [20] M. T. Tolley, S. M. Felton, S. Miyashita, L. Xu, B. Shin, M. Zhou, D. Rus, and R. J. Wood, "Self-folding shape memory laminates for automated fabrication," in *Intelligent Robots and Systems (IROS), 2013 IEEE/RSJ International Conference on*. IEEE, 2013, pp. 4931–4936.
- [21] M. T. Tolley, S. M. Felton, S. Miyashita, L. Xu, D. M. Aukes, D. Rus, and R. J. Wood, "Self-folding origami: shape memory composites activated by uniform heating," *Smart Materials and Structures*, vol. to be published, 2014.
- [22] B. Shin, S. M. Felton, M. T. Tolley, and R. J. Wood, "Self-assembling sensors for printable machines," in *Robotics and Automation (ICRA), 2014 IEEE International Conference on*. IEEE, 2014, pp. 4417–4422.
- [23] A. Lendlein and S. Kelch, "Shape-memory polymers," *Angewandte Chemie International Edition*, vol. 41, no. 12, pp. 2034–2057, 2002.
- [24] C. Liu, H. Qin, and P. Mather, "Review of progress in shape-memory polymers," *Journal of Materials Chemistry*, vol. 17, no. 16, pp. 1543–1558, 2007.
- [25] M. Yovanovich, J. Culham, and P. Teertstra, "Calculating interface resistance," *Electronics Cooling*, vol. 3, no. 2, pp. 24–29, 1997.
- [26] Z. Teoh and R. Wood, "A flapping-wing microrobot with a differential angle-of-attack mechanism," in *Robotics and Automation (ICRA), 2013 IEEE International Conference on*. IEEE, 2013, pp. 1381–1388.
- [27] A. T. Baisch and R. J. Wood, "Pop-up assembly of a quadrupedal ambulatory microrobot," in *Intelligent Robots and Systems (IROS), 2013 IEEE/RSJ International Conference on*. IEEE, 2013, pp. 1518–1524.
- [28] J. Gafford, S. Kesner, R. Wood, and C. Walsh, "Microsurgical devices by pop-up book mems," *ASME/IDETC: Robotics and Mechanisms in Medicine*, 2013.